Article type: Letter

Direct and label-free detection of the human Growth Hormone in urine by an ultrasensitive Bimodal Waveguide biosensor

Ana Belén González-Guerrero[1], *Jesús Maldonado*[1], *Stefania Dante*[1], *Daniel Grajales*[1], *and Laura M. Lechuga*[*,1]

*Corresponding Author: E-mail: laura.lechuga@icn2.cat

[1] Nanobiosensors and Bioanalytical Applications Group, Catalan Institute of Nanoscience and Nanotechnology (ICN2), CSIC, CIBER-BBN and The Barcelona Institute of Science and Technology, Campus UAB, Bellaterra, 08193 Barcelona, Spain.

Keywords: BiMW interferometer, silicon nanowaveguides, label-free biosensing, hGH detection, pg/mL detection range

A label-free interferometric transducer showing a detection limit for homogeneous sensing of 5×10^{-8} RIU, being equivalent to a protein mass coverage resolution of 2.8 fg mm^{-2}, is used to develop a high sensitive biosensor for protein detection. The extreme sensitivity of this transducer combined with a selective bioreceptor layer enables the direct evaluation of the human growth hormone (hGH) in undiluted urine matrix in the low pg mL^{-1} range.

1. Introduction

Interferometry has driven the development of highly sensitive detection techniques finding application in diverse scientific areas such as astronomy, seismology and metrology. In the field of nanobiotechnology, interferometric detection methods have prompted the development of ultrasensitive silicon-based integrated photonic biosensors. [1] These devices can consist of different arrangements such as Mach-Zehnder or Young configurations in which the confined light is split by Y-shaped waveguides into sensing and reference arms. The reported interferometric device with the highest sensitivity was based on a Young arrangement and reached a refractive index resolution of 6×10^{-8} RIU, corresponding to a protein mass coverage resolution of 20 fg mm^{-2}.[2] Furthermore, the mature silicon technology

industry allows the production of cost-effective waveguides since wafer-level fabrication drastically reduces the price per sensor.

Simultaneously, fundamental clinical research has provided a wide variety of biomarkers that can be employed for an early diagnosis, following of an illness progression and the application of personalized medicine. However, their wide use requires low-cost diagnostic tools. One of the factors that increase the cost of the analysis is the way of obtaining the sample. Although blood contains the highest concentration of specific biomarkers (some at ng mL^{-1}), its analysis requires the extraction of mL volumes by qualified personnel and is uncomfortable for patients. Urine is also an important source of biomarkers [3] and can be collected non-invasively, but the concentration of a particular biomarker in urine is normally very low (pg mL^{-1}).[4]

An important diagnostic biomarker, which is found at low concentration in urine, is the human Growth Hormone (hGH). Its evaluation is essential for the diagnosis of growth disorders by quantifying its secretion as either insufficient or overproduced. In addition, the extended use of hGH for sport doping makes necessary the implementation of new detection systems able to detect low quantities of hGH preferably in urine samples and in a user-friendly way. To detect hGH in urine at clinically relevant levels, different methodologies have already been developed but normally they require fluorescent or magnetic amplification. [5, 6] The most sensitive method to detect hGH in urine involves the use of hydrogel nanoparticles to concentrate urinary hGH obtaining detection limits (LOD) around pg mL^{-1}. [7-9] However, this method cannot be employed as a cost-effective and immediate hGH urine test due to the complexity of the steps undertaken.

Label-free optical biosensors can overcome most of the drawbacks of the conventional detection technologies. The most employed working mechanism of optical biosensors involves the evanescent field detection principle. Changes on the refractive index occurring at

the waveguide sensor surface affect some characteristics of the confined light (e.g. phase, intensity, and wavelength) that can be measured and correlated with such refractive index change. Optical biosensors operating by interferometric arrangement offer the highest sensitivity, [1] which is essential to avoid amplification or pre-concentration steps. Recently, we have developed a new concept of interferometric device, the Bimodal Waveguide interferometer (BiMW), which uses a straight waveguide to generate a two-mode interference of the same polarization.[10] In a BiMW device, the light (633 nm) is coupled into a nanorib waveguide (1.5 nm height and 4 μm wide) designed to achieve a high sensitivity while maintaining the single mode behavior in its longitudinal direction.[11] In addition, the height of the waveguide is tuned to propagate the fundamental mode in a single mode section and to excite the first transversal order in a bimodal section. An illustrative sketch of the sensing principle of the BiMW device can be seen in **Figure 1**. A sensor window is opened in the bimodal section, where the evanescent field of both modes interacts with the external medium. A specific bioreceptor layer with a refractive index n_0 is immobilized on the waveguide sensor surface. When a biorecognition process takes place in the sensor area of the device, the refractive index of the surface changes (n_0'). The variation of the external refractive index affects differently both modes causing them to travel at different velocities. At the end of the waveguide, the phase variation of the output light is directly related to the magnitude of the bio-interaction. Our preliminary work related to the BiMW has already demonstrated its extremely high sensitivity for bulk changes of the refractive index and for surface sensing [10] and the possibility of its integration in portable lab-on-a-chip platforms.[12] The bioreceptor layer plays a crucial role in the performance of a biosensor since it provides the selectivity for a particular analyte. Apart from affording irreversibility and long-term stability in fluid systems, the biofunctionalization protocol employed must preserve the surface from nonspecific interactions. Organofunctional silanes are usually employed to

supply silicon-derived surfaces with functional groups, among them, 3-aminopropyltriethoxysilane (APTES) has been the most employed in photonic devices.[13] The use of p-phenylenediisothiocyanate (PDITC) to activate amine groups (see **Figure S3**a) can avoid efficiently unspecific adsorptions since it can form compact monolayers by π-π stacking.[14] Recently, the extremely sensitivity of the BiMW biosensor for detecting miRNA has been reported using a similar biofunctionalisation procedure [17] demonstrating the versatility of the BiMW photonic device for biosensing.

In this work, we explore the high sensitivity of the BiMW transducer for the detection of extremely low concentrations of hGH directly from untreated and undiluted human urine samples.

2. Evaluation of the homogeneous and surface sensitivity

To first demonstrate the sensitivity of the BiMW transducer, a calibration curve was obtained by injections of different concentrations of HCl with different refractive indexes (0.024M, 0.049M, 0.097M, 0.242M and 0.483M) while keeping a continuous water flow. A previous refractive index evaluation was done with an ABBE Refractometer (Optic Ivymen System, Spain). For the calibration, phase variation is plotted versus index variation (Δn) (see Figure 2) and the obtained experimental sensitivity is $d(\varphi \times 2\pi)dn=2056$ ($R^2=0.998$). The noise of the system (s= 0.007%) has been taken as the signal deviation of the average during a baseline acquisition of n=100 points. The phase resolution is considered to be three times the S/N ration which is $1\times10^{-4}\times2\pi$ rad, corresponding to a refractive index resolution of the BiMW of only 5×10^{-8} RIU. It must be noticed that the LOD of the BiMW device is obtained by interpolation in the calibration curve. Since the commercial refractometer employed for knowing the refractive index of the HCl solutions has a resolution in the order of 10^{-4} RIU, this LOD is a theoretical estimation of the sensitivity of the sensor as it cannot be experimentally validated.

It is possible to calculate the resolution of the effective refractive index of the waveguide taking into account the interaction length of the device (l = 15 mm), the working wavelength (λ = 633 nm) and the phase resolution obtained before, following the equation:

$$\boldsymbol{\Delta N_{eff}} = \frac{\boldsymbol{\Delta\phi \cdot \lambda}}{\boldsymbol{2\pi \cdot l}} \qquad (1)$$

Obtaining a value for the minimum change of the N_{eff} of 4.2×10^{-9} RIU. Using this value and the parameters obtained by simulations (see SI, **Table S1**), and the relation given by: [15]

$$\boldsymbol{\Delta N_{eff}} = (\boldsymbol{\Delta z_c})^{-1} \frac{\boldsymbol{\delta N}}{\boldsymbol{\delta n_c}} \frac{\boldsymbol{dn}}{\boldsymbol{dc}} \boldsymbol{h\,\Delta\Gamma} \qquad \mathbf{(2)}$$

where ΔΓ is the surface coverage, h is approximated to 2 (see Ref [15] and SI) and the δn/δc is taken as 0.188 $cm^3\ g^{-1}$, [16] it is possible to calculate ΔΓ, using the mode TE_{10} which is more sensitive to surface changes (as demonstrated in Table S1), and obtaining a value of 2.8 fg mm^{-2}, which became the best value reported for a label-free photonic biosensor.

3. Evaluation of the sensitivity for the direct hGH detection

We have designed a direct immunoassay for the evaluation of hGH in both buffer medium and urine matrix. For that, the BiMW chip was covalently biofunctionalised with anti-hGH antibodies using a previous optimized functionalization protocol (see SI, **Figure S1**) and placed on the optical set-up (see SI, **Figure S2**). We performed triplicate measurements of concentrations of hGH ranging from 10 to 50 pg mL^{-1} and we adjusted the data to a fit model in all the range of concentrations, as shown in **Figure 3**a. The interaction between the antibody and the antigen was disrupted by the flow of a regeneration solution of HCl 0.1M which allows reusing the same biosensor up to eight times. The LOD was determined from the linear regression, as the concentration corresponding to the minimum measurable signal, set as three times the standard deviation of the blank signal. In this case, the LOD was found

to be 0.30 pg mL^{-1}. The specificity of the bioreceptor layer was demonstrated by injecting a non-target but related hormone (hTSH) at different concentrations (see Figure 3a, red circles). We also evaluated the ability of the BiMW transducer to detect hGH in 100% urine matrix. First, a non-spiked urine sample was injected to estimate the non-specific interactions coming from urine while maintaining PBST in a continuous flow (see Figure 3b). The recovery of the initial baseline at the end of the evaluation indicated the absence of non-specific adsorptions demonstrating the good non-fouling properties on the bioreceptor surface. Then, PBST was replaced by non-spiked urine as running buffer to avoid a complex interferometric signal due to the abrupt change of the refractive index of the solution when switching from buffer to urine in bulk. Spiked urine samples with different concentrations of hGH ranging from 0.1 to 1 ng mL^{-1} were evaluated (see Figure 3c). In Figure 3d, we show the phase variation versus the hGH concentration in urine. A linear response was obtained in all the range of concentrations evaluated. The LOD was calculated by linear fitting of the data, obtaining a value of only 3 pg mL^{-1}; this valued is one order of magnitude higher than the one obtained in buffer most likely caused by the partial denaturalization of the antibodies due to the urea present in the urine. The limit of quantification (LOQ) was considered as the concentration of target that causes a signal that corresponds to 10 times the N/S of the system showing the lowest concentration that could be quantified corresponding to 10 pg/mL. These results indicate that the BiMW biosensor would allow an extreme sensitive evaluation of hGH in pure urine samples in a label-free way.

4. Material and Methods

4.1 Chemical and reagents: Solvents for the device cleaning process: dry toluene, acetone, ethanol, hydrochloric acid (HCl, 35-38%), and methanol (MeOH) were supplied by Panreac (Barcelona, Spain). Nitric acid (69%) for chip oxidation, the silane (3-

aminopropyl)triethoxysilane (APTES), p-phenylenediisothiocyanate (PDITC), pyridine, N,N-Dimethylformamide (DMF), bovine serum albumin (BSA), albumin fluorescein isothiocyanate conjugate bovine (FTIC-BSA) and components for phosphate buffer saline (PBS/PBST); 10 mM phosphate, 2.9 mM KCl, 137 mM NaCl, Tween-20 1%, pH 7.4) and for carbonate buffer (0.1M Na_2CO_3, pH 9) were purchased from Sigma-Aldrich (Steinheim, Germany). Urine was obtained from healthy laboratory volunteers and was used without any further treatment. Recombinant human Growth Hormone (rhGH) composed exclusively of the 22 kDa isoform and thyroid stimulating hormone (hTSH) were provided by Dr. Parlow, National Hormone and Peptide Program (NHPP), National Institute of Diabetes and Digestive and Kidney Diseases (NIDDK, CA, USA). The monoclonal antibody (anti-hGH) which recognized the 22K and 20K hGH isoforms was obtained from and characterized by the Department of Immunology and Oncology from the National Center of Biotechnology (CNB-CSIC, Madrid, Spain). The anti-hGH was additionally purified by a HiTrap™ NHS-activated HP Column purchased from GE Healthcare (Uppsala, Sweden) previously prepared with rhGH and dialyzed by a PD-10 Desalting Column, both obtained from GE Healthcare (Uppsala, Sweden). The anti-hGH was injected into the column at a concentration of 4 mg mL^{-1}, obtaining 2.7 mL of purified antibody. This antibody solution was dialyzed; the resulting purified antibody was obtained at a concentration of 395 µg mL^{-1}. Purified antibody was aliquoted and stored at -20°C until its use. DI water from Millipore, USA, was used throughout. Polydimethylsiloxane (PDMS) was purchased from Dow Corning, Germany.

4.2 Si_3N_4 test surfaces: The Si_3N_4 test surfaces consisted of: a silicon dioxide layer (2 µm thickness) thermally grown over a silicon wafer (500 µm thickness), followed by a Si_3N_4 layer of 180 nm thickness deposited by low pressure chemical vapour deposition (LPCVD) technique. Wafer was diced into 1 cm^2 square pieces for the silanization experiments.

4.3 Analysis by atomic force microscopy: AFM images were recorded with an Agilent 5500 AFM/SPM microscope (formerly molecular Imaging PicoPlus AFM) in tapping mode. A multi-purpose low-coherence scanner with scan range up to 90 μm was used for imaging samples under ambient conditions. The AFM probes were NSC15 silicon pointprobes (force constant 30-50 N m^{-1}, resonant frequency 330 KHz) from MikroMasch, Estonia. AFM images processing was done with the WSxM software (Nanotec, Spain).

4.4 Fluorescent analysis: Fluorescence analysis of the patterned surfaces was carried out using an inverted microscope (TE 2000U Nikon, Spain) and a filter set for Cy3TM (Chroma Technology, USA). Images of the same experiment were taken with the same parameters of camera exposition for a reliable comparison.

4.5 Design and chip Fabrication: Optical waveguides employed in the design of the BiMW device were previously optimized for high surface sensitivity and a particular modal behavior in the visible range. They consisted of a Si_3N_4 core layer (n = 2.00) and a SiO_2 top and bottom cladding layer (n = 1.46). The devices were fabricated using silicon standard microelectronics technology at our Clean Room facilities. The fabricated wafer contained 12 chips of 30 × 10 mm^2 and each chip contained 16 BiMW devices with a pitch of 250 μm between them; the total length of the chip, including both single and bimodal parts, was 30 mm. The total length of the bimodal part was 25 mm, including the sensing window with a length of 15 mm and a width of 50 μm, placed 5 mm off the chip exit. Polishing of the chip edges was done with a Polishing Machine (Logitech CL50, UK) until an optical quality for end-coupling was achieved (0.3 μm).

4.6 Surface biofunctionalization of the sensor chips: The oxidized chips were biofunctionalised using previously optimized conditions (see Figure S1) i.e. immersion in a 1% APTES solution for 1 h and activated using 20 mM of PDITC. The chips were then incubated overnight in a solution of anti-hGH 50 µg mL^{-1} in carbonate buffer. The chips were then rinsed with PBS and water and immediately placed in the experimental set-up.

4.7 Detection of hGH in buffer: A direct immunoassay was employed for the evaluation of hGH in buffer. Prior to the measurements, a solution of BSA 2 mg mL^{-1} was flowed over the sensor surface to prevent nonspecific adsorption of protein in the tubing, sensor surface and flow cell. hGH solutions ranging from 10 to 50 pg mL^{-1} were prepared in triplicate in PBS by serial dilution starting from an original 1 mg mL^{-1} stock solution. PBS was used as running buffer during all the experiments. The volume of sample introduced was 250 µL in each case flowed at 30 µL min^{-1} over the sensor surface. A regeneration solution of HCl 100 mM was employed at 40 µL min^{-1} to recover the original bioreceptor surface after each measurement.

4.7 Detection of hGH in 100% urine: A direct immunoassay was employed for the evaluation of hGH in urine. In this case, a solution of BSA 2 mg mL^{-1} was also flowed over the sensor surface to prevent nonspecific adsorption. hGH solutions ranging from 0.1 to 1 ng mL^{-1} were prepared by spiking the urine with hGH. To evaluate the unspecific adsorption of non-spiked urine, PBST was used as running buffer and urine was injected at 30 µL min^{-1}. For the hGH evaluation, urine replaced PBST as running buffer. A regeneration solution of HCl 100 mM was employed at 40 µL min^{-1} to recover the original surface.

5. Conclusion

The performance of the BiMW biosensor for the ultrasensitive and fast detection of a biomarker as the hGH hormone at clinically relevant levels in urine samples has been

demonstrated in this work. To our knowledge, the established detection limit is the lowest ever reported for a label-free immunoassay in a complex matrix. The inherent label-free biosensor capabilities of the BiMW optical transducer, coupled with the unprecedented detection limits demonstrated herein establish the BiMW biosensor as a promising platform for direct, rapid and cost-effective clinical diagnosis.

Supporting Information

Additional supporting information may be found in the online version of this article at the publisher's website.

Table S1: Calculated sensitivities of the BiMW biosensor at λ=633 nm. For bulk sensitivity, aqueous buffer solution (n_{H2O} = 1.33) was employed. For surface sensitivity, a biolayer thickness of 10 nm was placed at the top of the waveguide. Optical parameters: $n_{cladding}$ = 1.33, n_{core} = 2.0, h_{core} = 340 nm, $n_{substrate}$ = 1.46, h_{rib} = 1.5 nm, w_{rib} = 4 µm, h_{bio} = 10 nm, n_{bio} = 1.45.

Figure S1: Silanization procedure of Si_3N_4 surfaces; a) sketch of the silanization procedure. Optimization of the silanization procedure: b) optimization of the silane concentration, c) optimization of the silanization time and d) optimization of the PDITC linker concentration.

Figure S2: Optical set-up employed for the evaluation of the BiMW chips. a) Image of a mounting of the sensor chip, b) scheme of the two-sectional photodiode employed to monitor the light exiting the waveguide and image of a real experiment showing the displacement of the light acquired by a CCD camera, c) position of the elements for the temperature control of the chip and d) PDMS flow cell fabricated by soft-lithography.

References

[1] M. C. Estevez, M. Alvarez, L. M. Lechuga *Laser & Photonics Reviews*. **2012**, 6, 463-487.
[2] A. Ymeti, J. Greve, P. V. Lambeck, T. Wink, S. W. van Hovell, T. A. Beumer, R. R. Wijn, R. G. Heideman, V. Subramaniam, J. S. Kanger *Nano Lett*. **2007**, 7, 394-397.
[3] J. Adachi, C. Kumar, Y. Zhang, J. V. Olsen, M. Mann *Genome Biol*. **2006**, 7.
[4] C. C. Saugy M, Rivier L, Brisson G, Ayotte C, Hemmersbach Haug PE, Segura J *Recent Advances in Doping analysis*. **1995**, 2.
[5] M. Bidlingmaier, J. Suhr, A. Ernst, Z. Wu, A. Keller, C. J. Strasburger, A. Bergmann *Clinical Chemistry*. **2009**, 55, 445-453.
[6] V. Serafín, N. Úbeda, L. Agüí, P. Yáñez-Sedeño, J. Pingarrón *Analytical and Bioanalytical Chemistry*. **2012**, 403, 939-946.
[7] J. Bosch, A. Luchini, S. Pichini, D. Tamburro, C. Fredolini, L. Liotta, E. Petricoin, R. Pacifici, F. Facchiano, J. Segura, E. Garaci, R. Gutierrez-Gallego *J Pharm Biomed Anal*. **2013**, 85, 194-197.
[8] C. Fredolini, D. Tamburro, G. Gambara, B. S. Lepene, V. Espina, E. F. Petricoin, 3rd, L. A. Liotta, A. Luchini *Drug Test Anal*. **2009**, 1, 447-454.
[9] A. Luchini, D. Tamburro, R. Magni, C. Fredolini, V. Espina, J. Bosch, E. Garaci, E. F. Petricoin, 3rd, L. A. Liotta *J Sports Med Doping Stud*. **2012**, 2.
[10] K. E. Zinoviev, A. B. Gonzalez-Guerrero, C. Dominguez, L. M. Lechuga *Lightwave Technology, Journal of*. **2011**, 29, 1926-1930.
[11] F. Prieto, B. Sepúlveda, A. Calle, A. Llobera, C. Domínguez, A. Abad, A. Montoya, L. M. Lechuga *Nanotechnology*. **2003**, 14, 907.
[12] D. Duval, A. B. Gonzalez-Guerrero, S. Dante, J. Osmond, R. Monge, L. J. Fernandez, K. E. Zinoviev, C. Dominguez, L. M. Lechuga *Lab on a Chip*. **2012**, 12, 1987-1994.
[13] M.-J. Bañuls, R. Puchades, Á. Maquieira *Analytica Chimica Acta*. **2013**, 777, 1-16.
[14] R. P. Gandhiraman, V. Gubala, N. C. Le, C. Volcke, C. Doyle, B. James, S. Daniels, D. E. Williams *Colloids and surfaces. B, Biointerfaces*. **2010**, 79, 270-275.
[15] W. Lukosz *Biosensors and Bioelectronics*. **1991**, 6, 215-225.
[16] A. Brandenburg, R. Krauter, C. Künzel, M. Stefan, H. Schulte *Appl. Opt.* **2000**, 39, 6396-6405.
[17] C. S. Huertas, D. Fariña, L. M. Lechuga *ACS Sensors*. **2016**, 1, 748-756.

Acknowledgements J. Maldonado and D. Grajales acknowledge the Mexican National Council for Science and Technology (CONACYT). The authors acknowledge the financial support from Project EPISENS of Spanish Ministry of Science and Innovation (TEC2012-34280) and HEPATOPOC project from CIBER-BBN. The nanoB2A is a consolidated research group (Grup de Recerca) of the Generalitat de Catalunya and has support from the Departament d'Universitats, Recerca i Societat de la Informació de la Generalitat de Catalunya (2014 SGR 624). ICN2 is the recipient of Grant SEV-2013-0295 from the "Severo Ochoa Centers of Excellence" Program of Spanish MINECO.

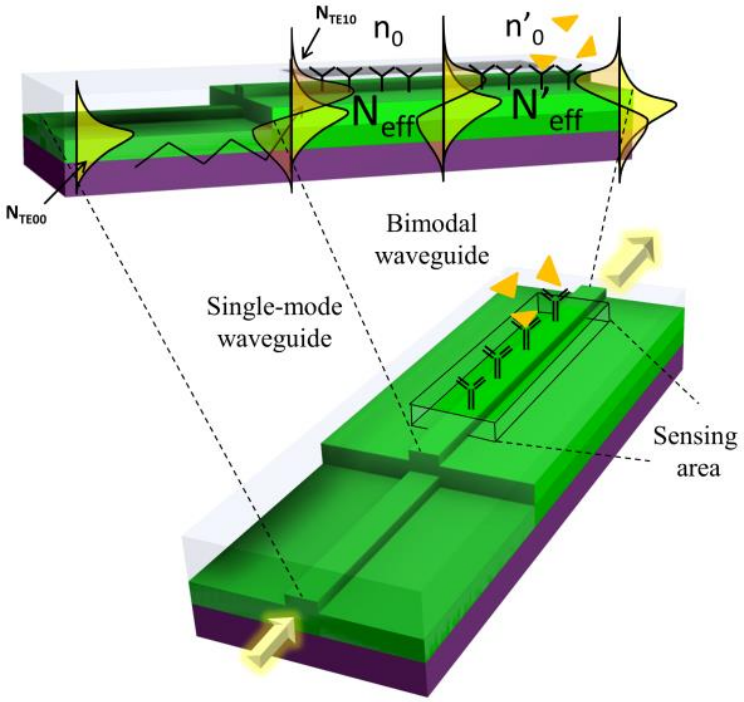

Figure 1. Sketch of a BiMW device. Light is coupled in a nanometric single mode waveguide in its fundamental mode; after some distance, the height of the waveguide increases allowing the simultaneous propagation of the fundamental and the first mode. Both modes interfere while interacting with the biological event taking place on the sensor area of the device. The different velocities of the travelling modes cause a phase variation that can be read-out at the end of the waveguide.

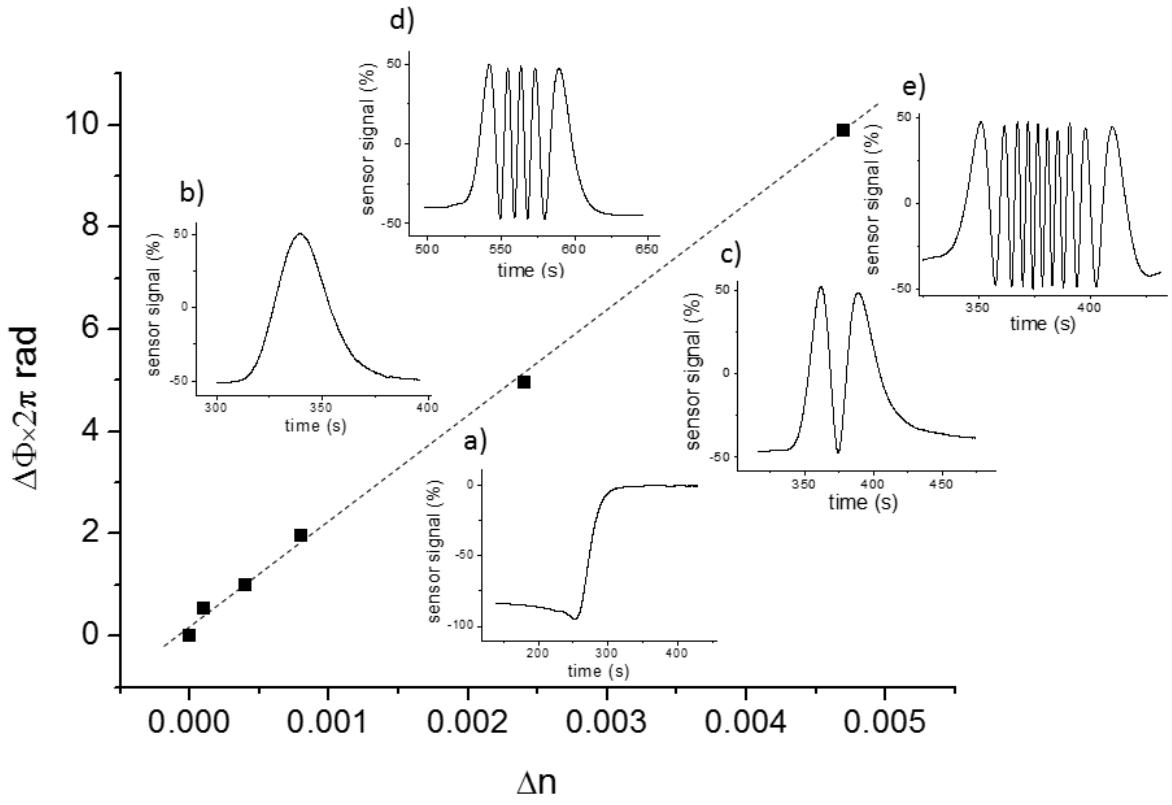

Figure 2. Calibration curve of the BiMW sensor obtained by evaluating the phase change as a function of the variation of the refractive index due to the injection of HCl concentrations. Inset: a) output signal for the detection of HCl 0.024M corresponding to a phase change of 0.53×2π rad, b) output signal for the detection of 0.049M corresponding to a phase change of 1×2π rad, c) output signal for the detection of 0.097M corresponding to a phase change of 1.97×2π rad, d) output signal for the detection of 0.242M corresponding to a phase change of 4.96×2π rad and e) output signal for the detection of 0.483M corresponding to a phase change of 9.90×2π rad.

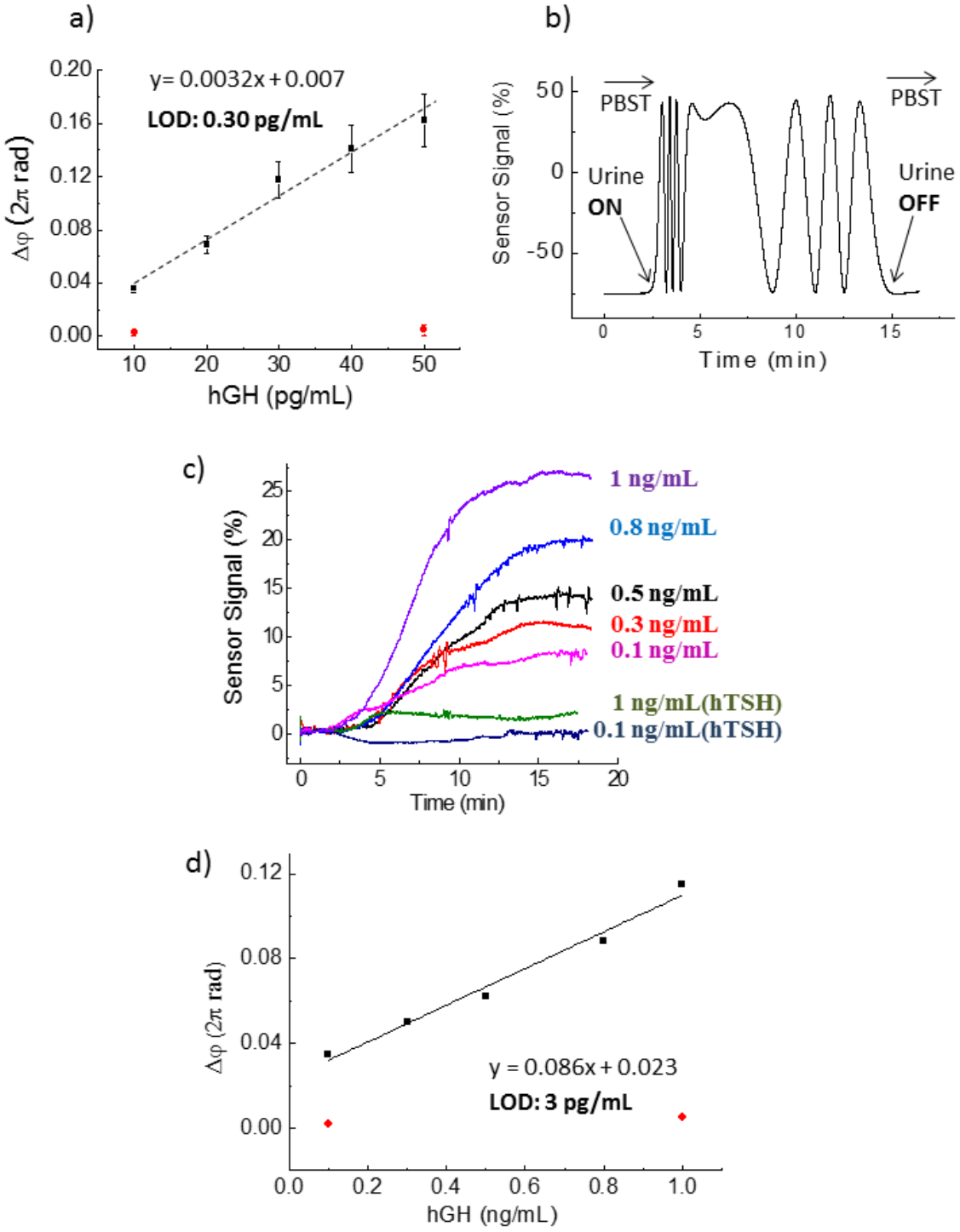

Figure 3. Biosensing evaluation of the presence of hGH in urine; a) calibration curve of hGH in PBS (black, squares) in comparison with non-specific hTSH target (red, circles), b) evaluation of non-specific adsorption of non-spiked urine on the biofunctionalised surface, c) real-time evaluation of urine samples spiked with different hGH concentrations and d)

calibration curve of hGH in urine (black, squares) in comparison with non-specific hTSH target (red, circles).

Graphical Abstract

Graphical abstract of the hGH direct detection using a bimodal nanometric waveguide in which anti-hGH are immobilizing on by a silane coupling agent.